

Supporting Information

Kinetics of Amyloid β monomer to oligomer exchange by NMR Relaxation

Nicolas L. Fawzi, Jinfa Ying, Dennis A. Torchia, and G. Marius Clore

Laboratory of Chemical Physics, National Institute of Diabetes and Digestive and Kidney Diseases, National Institutes of Health, Bethesda, Maryland 20892-0520

Supplementary Materials and Methods
Tables S1 to S4
Complete reference 10c from main text

Supplementary Materials and Methods

Sample preparation. Uniformly ^{15}N labeled A β (1-40) (rPeptide) was dissolved at 1 mg/ml in 3 mM NaOH with 50 mM NaOH added until solution pH reached 11. The final stock peptide concentration was determined by UV absorption at 280 nm with an extinction coefficient of $1490\text{ M}^{-1}\text{cm}^{-1}$. Aliquots of peptide stock sufficient for concentrations of 60 and 100 μM in a 500 μl volume were aliquoted in Eppendorf tubes, flash frozen in liquid nitrogen and lyophilized. Peptides were resolubilized in 3 mM Tris-HCl pH 8.0 and filtered/buffer exchanged to remove NaOH using a 2 ml Zeba desalting column (Pierce) equilibrated with 3 mM Tris-HCl pH 8.0. Exchanged samples were quantified by UV as above (yield of about 50% through the desalting column, as expected for a peptide below the exclusion limit of the Zeba column) and brought to the experimental conditions of $\sim 10\%$ $^2\text{H}_2\text{O}$, 50 mM HEPES pH 6.8 by adding 100 mM HEPES pH 6.3 with 20% $^2\text{H}_2\text{O}$ and 100 mM HEPES pH 6.8. This procedure was used to avoid the addition of acid or low pH solutions to set the pH of the samples, which in our experience can cause visible aggregation in the region of the solution where the acid is added.

NMR spectroscopy - $^1\text{H}_\text{N}$ - R_2 measurements. All experiments were performed at 10°C using Bruker 600 and 900 MHz spectrometers equipped with Bruker TCI z-axis gradient cryoprobes. Band selective ^1H pulses were applied throughout the experiments. A ^1H - ^{15}N HSQC-based 2D experiment was used to measure the residue specific $^1\text{H}_\text{N}$ - R_2 relaxation rate constants.^{S1} All 90° pulses in the INEPT and refocusing INEPT segments of the pulse sequence were of the E-BURP-2 or time reversed E-BURP-2 type^{S2} with pulse durations of 2.083 ms at 600 MHz and 1.4 ms at 900 MHz, centered at 8.25 ppm. An I-BURP-2 pulse (2.083 ms and 1.4ms at 600 and 900 MHz, respectively, centered at 8.25 ppm) was used for the ^1H decoupling pulse in the indirect ^{15}N dimension. ^1H R_2 relaxation decay curves were obtained by varying the length of the initial INEPT segment during which the ^1H and ^{15}N 180° pulses are applied such that the effective $^1\text{J}_{\text{N-H}}$ evolution time is kept constant.^{S1} For a peptide with its side chains protonated, it is important to use an amide proton selective ^1H 180° pulse for the RE-BURP profile (2.083 ms at 600 MHz and 1.4 ms at the 900 MHz, centered at 8.58 ppm) during the INEPT period, which leaves the $\text{H}\alpha$ protons unperturbed, thereby eliminating $^3\text{J}_{\text{HN-H}\alpha}$ modulation of the peak intensity. Typically, 6-8 variable relaxation delays were acquired in an interleaved manner, and the observed cross-peak intensity decays were fit to a two-parameter single exponential function to obtain the $^1\text{H}_\text{N}$ - R_2 rates.

NMR spectroscopy - Saturation transfer experiment. A ^1H saturation transfer experiment at 600 MHz was performed. A continuous wave (CW) pulse of 1.0 s duration at an RF power of either 350 Hz or 180 Hz at RF offsets ranging from 35 kHz to -35 kHz from the water resonance was applied to saturate the oligomer state and to allow saturation to transfer from the oligomer state to the monomeric peptide for readout. Immediately after the CW pulse, a jump-return scheme was used to optimize the excitation of the amide protons (centered at 8.36 ppm) while flipping the water back to the +z axis. A selective RE-BURP pulse (duration of 2.083 ms centered at 8.92 ppm at 600 MHz) sandwiched by two gradient pulses (sine-shaped, 300 μs at 42 G/cm) followed to further suppress the residual water peak after the excitation. The time domain data (2048 complex points, 110 ms acquisition time) were apodized by a squared cosine bell function and zero filled to 8096 complex points prior to Fourier transform using Bruker Topspin 2.1. The intensity attenuation of the $^1\text{H}_\text{N}$ envelope at each offset was measured as the slope of the best-fit line of the correlation plot of each spectrum with the reference spectrum obtained with no CW pulse applied.

Electron Microscopy (EM). Electron microscopy of negatively stained samples of A β (1-40) aggregates was performed essentially as described by Tycko and coworkers^{S3} with minor modification. Briefly, 2.5 μl of an NMR sample was placed on the carbon-coated side of a commercially available carbon film coated copper EM grid (Ultrathin Carbon Film/Holey Carbon, Ted Pella Inc.). After a 5 min adsorption period, solutions were blotted, washed three times with 5 μL deionized water for 5 s and blotted. 5 μL of

3% uranyl acetate was applied for 60 s, blotted, and the sample air-dried. Images were acquired as described.^{S3}

Dynamic Light Scattering (DLS). Dynamic light scattering was performed using a Zetasizer Nano instrument (Malvern). Samples were diluted 10-fold in NMR buffer at 4°C, placed in a 10°C equilibrated quartz cuvette (50 μ l sample size) and immediately introduced into the DLS instrument for a 1 min temperature equilibration, and then scanned. Default and auto adjust parameters were used for data acquisition.

McConnell model for saturation transfer. Data from the saturation transfer experiment were modeled with a homogenous form of the McConnell equations^{S4} as presented in Eq. [21] of Helgstrand et al.^{S5} describing a single spin in two-site exchange at chemical equilibrium between an observable state with low R_2 and an oligomer bound state with larger R_2 in the presence of a CW RF field. The single spin McConnell model used by Helgstrand et al. was extended to incorporate cross-relaxation between two spins separated by 2.5 kHz, one representing the observed amide protons, and the other representing aliphatic protons coupled by cross-relaxation. The expansion of the model to two spins with different resonance frequencies was necessary to account for the \sim 5 kHz width (at half height) of the saturation profile observed for the 60 μ M sample (black circles in Figure 6 of main text) where the fraction of oligomers is negligible (cf. Figure 1B of main text). The width of the profile, which spans the ^1H chemical shift range of the monomer, is ascribed to saturation transfer arising from cross-relaxation among protons in the monomer. The full magnetization matrix is then given by:

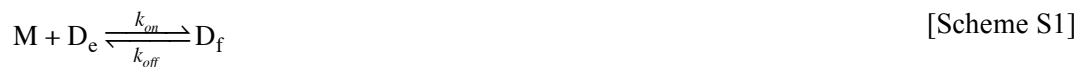
$$\frac{d}{dt} \begin{bmatrix} E/2 \\ I_x^A \\ I_y^A \\ I_z^A \\ I_x^B \\ I_y^B \\ I_z^B \\ S_x^A \\ S_y^A \\ S_z^A \\ S_x^B \\ S_y^B \\ S_z^B \end{bmatrix} = \begin{bmatrix} 0 & 0 & 0 & 0 & 0 & 0 & 0 & 0 & 0 & 0 & 0 & 0 & 0 & 0 \\ 0 & \lambda_I^A + k_{on}^{app} & \Omega_I^A & -\omega_y & -k_{off} & 0 & 0 & 0 & 0 & 0 & 0 & 0 & 0 & 0 \\ 0 & -\Omega_I^A & \lambda_I^A + k_{on}^{app} & \omega_x & 0 & -k_{off} & 0 & 0 & 0 & 0 & 0 & 0 & 0 & 0 \\ -2\Theta_I^A & \omega_y & -\omega_x & \rho_I^A + k_{on}^{app} & 0 & 0 & -k_{off} & 0 & 0 & 0 & \sigma_A & 0 & 0 & 0 \\ 0 & -k_{on}^{app} & 0 & 0 & \lambda_I^B + k_{on}^{app} & \Omega_I^B & -\omega_y & 0 & 0 & 0 & 0 & 0 & 0 & 0 \\ 0 & 0 & -k_{on}^{app} & 0 & -\Omega_I^B & \lambda_I^B + k_{on}^{app} & \omega_x & 0 & 0 & 0 & 0 & 0 & 0 & 0 \\ -2\Theta_I^B & 0 & 0 & -k_{on}^{app} & \omega_y & -\omega_x & \rho_I^B + k_{on}^{app} & 0 & 0 & 0 & 0 & 0 & 0 & \sigma_B \\ 0 & 0 & 0 & 0 & 0 & 0 & 0 & \lambda_S^A + k_{on}^{app} & \Omega_I^S & -\omega_y & -k_{off} & 0 & 0 & 0 \\ 0 & 0 & 0 & 0 & 0 & 0 & 0 & -\Omega_I^S & \lambda_S^A + k_{on}^{app} & \omega_x & 0 & -k_{off} & 0 & 0 \\ -2\Theta_S^A & 0 & 0 & \sigma_A & 0 & 0 & 0 & \omega_y & -\omega_x & \rho_S^A + k_{on}^{app} & 0 & 0 & 0 & -k_{off} \\ 0 & 0 & 0 & 0 & 0 & 0 & 0 & -k_{on}^{app} & 0 & 0 & \lambda_S^B + k_{on}^{app} & \Omega_I^B & -\omega_y & 0 \\ 0 & 0 & 0 & 0 & 0 & 0 & 0 & 0 & -k_{on}^{app} & 0 & -\Omega_I^B & \lambda_S^B + k_{on}^{app} & \omega_x & 0 \\ -2\Theta_S^B & 0 & 0 & 0 & 0 & 0 & \sigma_B & 0 & 0 & -k_{on}^{app} & \omega_y & -\omega_x & \rho_S^B + k_{on}^{app} & 0 \end{bmatrix} \times \begin{bmatrix} E/2 \\ I_x^A \\ I_y^A \\ I_z^A \\ I_x^B \\ I_y^B \\ I_z^B \\ S_x^A \\ S_y^A \\ S_z^A \\ S_x^B \\ S_y^B \\ S_z^B \end{bmatrix}$$

[Eq. S1]

where I and S represent the magnetizations of the spins representing the amide and aliphatic protons, respectively, in free or oligomer bound states A or B, respectively. The relaxation rates for transverse and longitudinal magnetization are λ and ρ , respectively; σ is the cross-relaxation rate between spins I and S ; Ω is the resonance offset frequency and ω the strength of the RF field applied along the appropriate axis; E is unity; and Θ is related to the equilibrium magnetization as described in ref. S5. The cross-relaxation rate in the monomeric form, σ_A , is assumed to be small and the best-fit parameters do not change with rates over a large range of values (from -0.5 to -3.0 s^{-1}), where the only effect is a slightly broader on-resonance saturation peak with increasingly negative values of σ_A . The rate in the oligomer bound form, σ_B , is assumed to be large (-500 s^{-1}). The exact value of σ_B has no effect on the fitted λ_B value (the R_2 rate for the oligomer bound species) since the I and S spins are equivalently affected by off-resonance pulses when R_2 is large. The numerical solution for I_z^A , the experimentally observed magnetization, after a given

saturation time as a function of offsets was calculated using the matrix exponential function present in Matlab. The experimental saturation profiles were best-fit to Eq. [S1] excluding the region near-resonance with $|\text{RF offset}| \leq 2.5$ kHz as this region of the profiles is not well represented by the model due to the many-spin nature of the system.

Equilibrium Binding model. A phenomenological second order equilibrium binding model for the association of monomeric peptide to oligomer can be represented as follows:



where $[M]$, $[D_e]$ and $[D_f]$ are the concentrations of free monomer, the empty sites in the ‘dark’ state, and the filled binding sites in the ‘dark’ state, respectively; and k_{on} and k_{off} are second order association and first order dissociation rate constants, respectively. At equilibrium

$$k_{on}[M][D_e] = k_{off}[D_f] \quad [\text{Eq. S2}]$$

We note that $[D_e] + [D_f] = [D_T]$, where $[D_T]$ is the concentration of the total number of binding sites in the dark state, so

$$k_{on}[M]([D_T] - [D_f]) = k_{off}[D_f] \quad [\text{Eq. S3}]$$

Defining

$$k_{on}^{app} = k_{on}([D_T] - [D_f]) \quad [\text{Eq. S4}]$$

as the apparent pseudo-first order association rate constant, we obtain

$$k_{on}^{app} [M] = k_{off}[D_f] \quad [\text{Eq. S5}]$$

which is equivalent to Scheme 1 in the main text where M and D_f are referred to as M_{free} and M_{bound} , respectively. If $k_{off} \gg k_{on}^{app}$, $[M] \gg [D_f]$ and therefore only a small concentration of monomer is involved in transient binding to oligomer. Consequently, $^1\text{H}_N$ resonances with the small R_2^{dark} rates (300 s^{-1}) will make a negligible contribution to a standard 1D ^1H -NMR spectrum, such that only the $^1\text{H}_N$ resonances of the free monomer are observed.

Supplementary references

- (S1) Iwahara, J.; Tang, C.; Clore, G. M. *J. Magn. Reson.* **2007**, *184*, 185-195.
- (S2) Geen, H.; Freeman, R. *J. Magn. Reson.* **1991**, *93*, 93-141.
- (S3) Chen, B.; Thurber, K. R.; Shewmaker, F.; Wickner, R. B.; Tycko, R. *Proc. Natl. Acad. Sci. U. S. A.* **2009**, *106*, 14339-14344.
- (S4) McConnell, H.M. *J. Chem. Phys.* **1958**, *28*, 430-431.
- (S5) Helgstrand, M.; Hard, T.; Allard, P. *J. Biomol. NMR* **2000**, *18*, 49-63.

Table S1. ^{15}N - R_2 rates and standard deviations (s.d.) measured at 900 MHz for 60, 150 and 300 μM $\text{A}\beta(1-40)$ samples.

Residue Number	Total $\text{A}\beta(1-40)$ concentration					
	60 μM		150 μM		300 μM	
	R_2 (s^{-1})	s.d. (s^{-1})	R_2 (s^{-1})	s.d. (s^{-1})	R_2 (s^{-1})	s.d. (s^{-1})
3	3.79	0.04	4.07	0.05	5.43	0.04
4	4.14	0.04	4.53	0.05	6.03	0.04
5	5.35	0.07	5.85	0.08	7.30	0.07
7	9.60	0.17	9.33	0.17	11.59	0.15
8	9.12	0.15	9.16	0.16	10.93	0.14
9	7.33	0.10	7.58	0.11	9.34	0.11
10	5.63	0.06	6.28	0.07	7.91	0.08
11	5.92	0.07	6.61	0.09	8.51	0.09
12	5.87	0.07	6.53	0.08	8.36	0.08
13	12.28	0.26	12.12	0.27	14.57	0.28
15	15.55	0.42	15.02	0.45	17.70	0.52
16	8.14	0.13	8.75	0.15	10.92	0.16
17	6.21	0.09	7.09	0.11	9.26	0.12
18	5.58	0.07	6.52	0.09	8.43	0.10
19	5.94	0.08	6.82	0.10	9.09	0.12
20	6.02	0.08	6.92	0.10	8.8	0.11
21	5.41	0.07	6.38	0.09	8.12	0.09
22	4.95	0.05	5.74	0.07	7.62	0.07
23	5.14	0.06	5.83	0.06	7.61	0.07
24	4.63	0.05	5.23	0.05	6.87	0.06
25	6.02	0.07	6.36	0.07	8.03	0.08
26	7.19	0.09	7.68	0.10	9.04	0.09
27	10.47	0.21	11.18	0.21	12.39	0.19
28	6.95	0.09	7.09	0.09	9.01	0.10
29	6.00	0.07	6.40	0.08	8.22	0.08
30	4.59	0.05	5.13	0.06	6.73	0.06
31	4.12	0.04	4.80	0.05	6.63	0.06
32	4.55	0.05	5.27	0.06	6.96	0.06
33	4.95	0.05	5.54	0.07	7.41	0.07
34	4.06	0.05	4.76	0.05	6.52	0.06
35	4.20	0.05	4.92	0.06	6.66	0.06
36	3.48	0.04	4.15	0.04	5.79	0.05
37	4.51	0.05	5.00	0.05	6.70	0.06
38	3.64	0.04	4.11	0.05	5.45	0.05
39	2.45	0.03	2.84	0.03	4.43	0.03
40	2.22	0.04	2.70	0.04	3.79	0.04

Table S2. ^{15}N - R_2 rates and standard deviations (s.d.) measured at 600 MHz for 60, 150 and 300 μM $\text{A}\beta(1-40)$ samples.

Residue Number	Total $\text{A}\beta(1-40)$ concentration					
	60 μM		150 μM		300 μM	
	R_2 (s^{-1})	s.d. (s^{-1})	R_2 (s^{-1})	s.d. (s^{-1})	R_2 (s^{-1})	s.d. (s^{-1})
3	3.46	0.02	3.81	0.02	4.93	0.04
4	3.61	0.02	4.15	0.02	5.31	0.04
5	4.85	0.03	5.20	0.04	6.34	0.08
7	8.98	0.23	8.86	0.15	10.6	0.28
8	8.32	0.13	8.55	0.14	10.1	0.25
9	6.57	0.07	6.83	0.08	8.07	0.14
10	4.79	0.03	5.43	0.04	6.91	0.10
11	5.02	0.03	5.79	0.05	7.15	0.11
12	4.89	0.03	5.67	0.04	7.13	0.11
13	10.42	0.25	10.90	0.27	11.61	0.49
15	14.51	0.47	13.96	0.54	16.39	1.01
16	7.19	0.09	7.96	0.11	9.66	0.25
17	5.34	0.04	6.33	0.07	8.12	0.17
18	4.66	0.03	5.70	0.05	7.38	0.13
19	5.07	0.04	6.17	0.06	7.89	0.15
20	5.15	0.04	6.19	0.06	8.04	0.16
21	4.82	0.03	5.80	0.07	7.43	0.12
22	4.32	0.03	5.16	0.03	6.59	0.09
23	4.52	0.03	5.34	0.03	6.87	0.09
24	3.83	0.03	4.53	0.02	5.96	0.05
25	5.14	0.03	5.72	0.04	7.06	0.10
26	6.64	0.06	7.09	0.08	8.41	0.15
27	9.52	0.19	10.00	0.23	10.78	0.36
28	6.41	0.06	6.73	0.07	8.32	0.15
29	5.44	0.04	5.71	0.04	7.07	0.10
30	3.93	0.03	4.55	0.03	5.98	0.07
31	3.63	0.03	4.28	0.02	5.97	0.07
32	3.93	0.02	4.75	0.03	6.37	0.08
33	4.43	0.03	5.20	0.04	6.81	0.09
34	3.47	0.02	4.25	0.03	5.82	0.07
35	3.78	0.03	4.45	0.03	6.05	0.08
36	3.01	0.02	3.77	0.02	5.17	0.05
37	4.10	0.03	4.75	0.03	6.15	0.07
38	3.17	0.02	3.63	0.02	5.01	0.04
39	2.06	0.01	2.57	0.01	3.82	0.03
40	1.72	0.01	2.31	0.02	3.70	0.03

Table S3. $^1\text{H}_\text{N}$ - R_2 rates and standard deviations (s.d.) measured at 900 MHz for 60, 150 and 300 μM $\text{A}\beta(1-40)$ samples.

Residue Number	Total $\text{A}\beta(1-40)$ concentration					
	60 μM		150 μM		300 μM	
	R_2 (s^{-1})	s.d. (s^{-1})	R_2 (s^{-1})	s.d. (s^{-1})	R_2 (s^{-1})	s.d. (s^{-1})
3	6.61	0.05	7.10	0.04	8.81	0.03
4	7.46	0.05	8.12	0.04	9.76	0.04
5	9.96	0.07	10.44	0.05	12.23	0.05
7	17.76	0.18	17.53	0.12	19.44	0.19
8	16.96	0.17	17.20	0.12	18.85	0.17
9	13.42	0.11	13.88	0.08	15.84	0.09
10	9.94	0.08	10.81	0.06	12.57	0.06
11	11.11	0.08	12.03	0.06	13.57	0.06
12	11.13	0.08	12.12	0.06	14.01	0.06
13	22.91	0.32	22.71	0.22	25.03	0.30
15	26.93	0.51	26.49	0.32	28.46	0.44
16	15.73	0.14	16.23	0.10	18.63	0.18
17	11.95	0.10	13.16	0.08	15.34	0.10
18	11.72	0.09	12.99	0.07	14.69	0.08
19	11.52	0.09	12.98	0.08	14.79	0.09
20	11.55	0.10	12.80	0.08	14.65	0.08
21	10.12	0.08	11.15	0.06	13.03	0.07
22	9.12	0.06	10.18	0.05	11.90	0.05
23	9.60	0.07	10.57	0.05	12.18	0.05
24	8.39	0.06	9.250	0.04	10.95	0.04
25	10.63	0.07	11.41	0.05	12.95	0.05
26	12.76	0.11	13.03	0.07	14.61	0.08
27	19.48	0.23	19.99	0.16	20.30	0.23
28	12.47	0.10	12.72	0.07	14.45	0.07
29	10.89	0.07	11.52	0.05	13.22	0.06
30	7.45	0.06	8.22	0.05	9.90	0.05
31	7.93	0.05	8.79	0.04	10.62	0.04
32	8.31	0.05	9.34	0.04	11.14	0.04
33	9.63	0.06	10.51	0.05	12.46	0.05
34	7.32	0.06	8.12	0.05	9.89	0.05
35	7.67	0.06	8.58	0.05	10.32	0.05
36	6.25	0.05	7.15	0.03	8.80	0.04
37	8.40	0.06	9.17	0.04	10.87	0.04
38	6.33	0.05	7.07	0.04	8.81	0.04
39	4.06	0.04	4.74	0.02	6.31	0.03
40	3.33	0.04	3.97	0.03	5.49	0.03

Table S4. $^1\text{H}_\text{N}$ - R_2 rates and standard deviations (s.d.) measured at 600 MHz for 60, 150 and 300 μM $\text{A}\beta(1-40)$ samples.

Residue Number	Total $\text{A}\beta(1-40)$ concentration					
	60 μM		150 μM		300 μM	
	R_2 (s^{-1})	s.d. (s^{-1})	R_2 (s^{-1})	s.d. (s^{-1})	R_2 (s^{-1})	s.d. (s^{-1})
3	6.55	0.14	7.03	0.06	9.04	0.12
4	7.03	0.15	7.98	0.06	9.57	0.14
5	9.85	0.22	10.37	0.09	12.01	0.20
7	17.55	0.66	17.54	0.24	18.93	0.71
8	14.76	0.33	16.85	0.20	17.83	0.55
9	13.00	0.24	13.60	0.10	15.31	0.26
10	9.09	0.21	10.22	0.09	12.31	0.21
11	10.06	0.20	10.89	0.09	13.01	0.22
12	10.30	0.19	11.19	0.09	13.66	0.23
13	18.50	0.90	21.20	0.42	24.67	1.03
15	25.58	1.65	24.75	0.68	26.36	1.63
16	14.55	0.29	15.74	0.15	17.80	0.59
17	11.61	0.24	12.80	0.11	14.44	0.33
18	10.53	0.22	11.83	0.10	13.82	0.28
19	10.78	0.23	12.15	0.10	14.33	0.30
20	11.08	0.24	12.28	0.11	13.91	0.31
21	10.12	0.20	10.55	0.13	12.57	0.22
22	8.51	0.17	9.70	0.08	11.49	0.18
23	8.75	0.17	10.18	0.07	12.08	0.18
24	7.46	0.14	8.71	0.06	10.82	0.14
25	10.09	0.18	11.18	0.08	12.96	0.18
26	12.16	0.26	13.29	0.11	14.98	0.30
27	19.34	0.88	19.59	0.36	19.36	1.24
28	12.35	0.24	12.71	0.10	14.23	0.26
29	10.64	0.19	11.38	0.08	12.71	0.19
30	7.09	0.18	7.87	0.08	9.87	0.17
31	7.39	0.13	8.61	0.06	10.76	0.14
32	7.92	0.15	8.88	0.06	11.11	0.16
33	8.92	0.17	10.06	0.08	12.09	0.17
34	6.85	0.17	7.94	0.08	9.87	0.18
35	7.82	0.18	8.61	0.08	10.28	0.18
36	5.73	0.14	6.95	0.06	8.99	0.15
37	8.42	0.16	8.94	0.07	10.83	0.14
38	6.31	0.13	6.83	0.06	8.71	0.13
39	3.91	0.13	4.64	0.05	6.45	0.10
40	3.04	0.14	4.01	0.06	5.72	0.09

Complete Reference 10c in the main text

Yu, L.; Edalji, R.; Harlan, J. E.; Holzman, T. F.; Lopez, A. P.; Labkovsky, B.; Hillen, H.; Barghorn, S.; Ebert, U.; Richardson, P. L.; Miesbauer, L.; Solomon, L.; Bartley, D.; Walter, K.; Johnson, R. W.; Hajduk, P. J.; Olejniczak, E. T. *Biochemistry* **2009**, *48*, 1870-1877.